# The effects of glycation on the composition, metabolism and barrier function of epidermal lipids

Mami Yokota and Yoshihiro Tokudome*

Laboratory of Dermatological Physiology, Faculty of Pharmaceutical Sciences, Josai University, 1-1 Keyakidai, Sakado, Saitama 350-0295, Japan

* Corresponding author at: Faculty of Pharmaceutical Sciences, Josai University, 1-1 Keyakidai, Sakado, Saitama 350-0295, Japan.

Tel and Fax: +81 49 271 8140

E-mail: tokudome@josai.ac.jp

**KEYWORDS**

advanced glycation end products, epidermal lipids, fatty acid, barrier function

***Short title***: Relationship between AGEs and epidermal lipids metabolism

**ABSTRACT**

***Background/Aims:*** Advanced glycation end products (AGEs), which are linked to both aging and hyperglycemia, cause marked functional and structural alterations in human skin. The metabolism of glucose is closely associated with that of fatty acids (FAs), which share the same energy yielding reaction pathways; however, the effects of AGEs on epidermal FA metabolism remain unclear. ***Methods:*** Ceramide, cholesterol and FA content in a reconstructed epidermal model glycated by glyoxal was analyzed by high performance thin layer chromatography. FA species extracted from HaCaT keratinocytes were identified by gas chromatography-mass spectrometry. Regulation of FA synthesis was analyzed by real-time PCR. For physical analysis, excised mouse skin was glycated using a vertical diffusion cell and used for evaluation of barrier function by assessment of transepidermal water loss and observation of sodium fluorescein penetration. ***Results:*** Saturated FA content was significantly increased in glycated epidermis, and glycation upregulated mRNA expression of FA elongase 2 and 3 and FA synthase in HaCaT cells. Furthermore, both inside-out and outside-in barrier functions were disrupted in glycated, excised skin. ***Conclusion:*** Biological and physical changes

in the epidermis, especially the upregulation of FA synthesis by glycation, contributed to barrier disruption.

## INTRODUCTION

Advanced glycation end products (AGEs), which are generated via the non-enzymatic Maillard reaction between the aldehyde group of reducing sugars and amino group of proteins, lipids or nucleic acids [1, 2], accumulating in aged or diabetes-conditioned tissue [3, 4] AGEs have been detected in both the epidermis and dermis [4, 5] and cause significant functional and structural alterations in human skin. Since striking characteristics of AGEs, yellowish tint and autofluorescence affect skin appearance, anti AGEs strategy to skin attract much attention in recent years. Epidermal glycation causes decrease in water content of the stratum corneum (SC) and glycation of collagen and elastic fibers is considered as one of the causes of degradation of dermal extra cellular matrix [6, 7, 8] . Additionally, AGEs also induce biological reactions via binding to the receptor for AGEs (RAGE) [9]. RAGE signal transduction induces activation of nuclear factor kappa B (NF-κB) and subsequent transcription of proinflammatory genes, including interleukin 1 (IL-1), tumor necrosis factor alpha (TNFα), matrix metalloproteinases (MMPs) and RAGE itself, accelerating further skin senescence and deconstruction [10, 11]

The metabolism of glucose is closely associated with that of fatty acids (FAs) because both substrates share the same energy yielding reaction pathways, which involve the accumulation of acetyl CoA. Recent studies show that excess lipid accumulation in non-adipose tissue is associated with cytotoxicity [12, 13]. FAs are simple lipids, which form part of phospholipids, triacylglycerol and ceramides, and exist ubiquitously in cells as essential constituents of the cell membrane and as important substrates for energy metabolism. FAs are produced by degradation of more complex lipids or are newly synthesized from the conversion of Acetyl-CoA/Malonyl-CoA to palmitic acid by fatty acid synthase (FASN). The fatty acid elongase (ELOVL) family of proteins is the most well characterized group of enzymes for FA elongation in the generation of very long chain fatty acids [14]. Interestingly, the SC has a unique lipid composition: it consists of FA, ceramides (CERs) and cholesterol (CHOL) in an approximately equimolar ratio. These lipids have an essential role in the barrier function of the skin and are produced in viable epidermis.

Despite the strong relationship between glucose and FA metabolism, the effects of glycation on skin FAs and barrier function are currently not well studied. Thus,

we focused on the relationship between glycation and intercellular lipids and glycation's effect on the barrier function of the skin.

In this study, we determined that FA content was increased via upregulation of *FASN* and *ELOVL* expression by glycation of epidermal keratinocytes. Furthermore, changes in the ratio of epidermal lipid components, as well as structural alterations, resulted in barrier disruption in skin.

## MATERIALS AND METHODS

### *Reagents*

Glyoxal (GO), cholesterol and palmitic acid were purchased from Wako Pure Chemical Industries, Ltd. (Osaka, Japan). An antibody specific for AGEs (6D12) was purchased from TransGenic Inc. (Fukuoka, Japan). Alexa 546-conjugated secondary antibody was purchased from Life Technologies (Carlsbad, CA, USA). Thiazolyl blue tetrazolium bromide (MTT) was purchased from Sigma-Aldrich (St. Louis, MO, USA). For lipid standards, ceramide NS and AS were purchased from Matreya (State College, PA, USA) and ceramide NP and AP were purchased from Evonic Industries AG (Essen,

Germany). Gas chromatography-mass spectrometry standard F.A.M.E. Mix RM-3 was purchased from Sigma-Aldrich.

*Cell culture*

The immortalized human skin keratinocyte cell line HaCaT was maintained in Dulbecco's modified Eagle's medium (DMEM) supplemented with 10% fetal bovine serum and incubated in a humidified atmosphere of 5% $CO_2$ at 37°C. AGEs were induced by GO. After 30 min of exposure to GO in culture medium, cells were washed twice with culture medium and fresh culture medium added.

The reconstructed epidermal model (Labcyte EPIMODEL) was purchased from JTEC (Gamagori, Japan) and maintained in the supplied culture medium. AGEs were induced by exposure to various concentrations of GO for 72 h from the basal side.

*Cell viability assay*

HaCaT keratinocytes were cultured for 24 h before exposure to various concentrations of GO. After 48 h incubation, cells were washed and incubated with 0.5

mg/mL MTT in culture medium for a further 4 h. The resulting formazan crystals were solubilized in 150 μL of 0.04 M hydrochloric acid/isopropyl alcohol. The absorbance at 570 nm was measured using a microplate reader (SpectraMax M2$^{e}$; Molecular Devices, Sunnyvale, CA, USA).

*RNA extraction and quantitative real time PCR*

Total RNA was isolated from HaCaT cells using RNAiso Plus (Takara Bio, Otsu, Japan), followed by reverse transcription to cDNA using PrimeScript® RT reagent kit (Takara Bio) using a thermal cycler (Veriti; Applied Biosystems, Foster City, CA, USA). Real-time PCR reactions were performed using SYBR® *Premix Ex Taq*™ (Takara Bio) using a StepOnePlus™ analyzer (Applied Biosystems) with the indicated primers (Table S1). The fold-change of expression was calculated according to the $\Delta\Delta C_T$ method using glyceraldehyde-3-phosphate dehydrogenase (GAPDH) as an endogenous control.

*Immunocytochemistry*

HaCaT cells were cultured on glass slides (Fisher Scientific UK Ltd., Loughborough,

UK) prior to the induction of glycation with GO. After 48 h incubation, cells were washed twice with PBS and fixed with ice cold methanol for 15 min at −30°C. Nonspecific staining was blocked by pre-incubation with 1% bovine serum albumin in PBS for 1 h at room temperature. For primary antibody reactions, cells were incubated with the antibody against AGEs at a 1:200 dilution in Can Get Signal immunostain® Solution A (Toyobo, Osaka, Japan) overnight at 4°C. Bound antibodies were visualized with Alexa 546-conjugated secondary antibody at a 1:200 dilution in Can Get Signal immunostain® solution A for 1 h at room temperature. After washing, Hoechst 33258 (Dojindo Laboratories, Mashiki, Japan) was added for nuclear counterstaining. All images were obtained using an IX71 microscope (Olympus, Tokyo, Japan).

*Lipid extraction*

For lipid extraction from HaCaT cells, $4 \times 10^5$ cells were plated on 6 cm plates. 48 h after exposure to GO, lipids were extracted according to the method of Bligh and Dyer with slight modifications [15]. Briefly, cells were washed and scraped from dishes into 1.2 mL of $ddH_2O$. To lyse cells completely, cell suspensions were sonicated. The protein

content of the lysate was quantified by the conventional Lowry method. Three mL of each of $CHCl_3$ and MeOH were added to the cell suspension before further sonication. Then samples were filtrated and 1.5 mL of $ddH_2O$ added, followed by centrifugation at 215 *g* for 20 min. The lower layer was collected and dried under a $N_2$ stream and used as lipid samples.

Epidermal lipid samples from the reconstructed epidermal model were extracted in $CHCl_3$/MeOH 2:1 (v/v) solution after being washed and excised from the transwell. Samples were minced, sonicated for 10 min, and then the solution filtered and dried under a $N_2$ stream. All lipid extracts and standards were dissolved in $CHCl_3$/MeOH 2:1 (v/v) solution.

*High performance thin-layer chromatography (HPTLC) analysis*

10 μL of lipid extracts were applied to the HPTLC plate (HPTLC silica gel 60, Merck KGaA; Darmstadt, Germany) together with lipid standards to generate calibration curves and the plate was developed twice in a saturated chromatographic chamber containing $CHCl_3$/MeOH/$CH_3COOH$ 190:9:1 (v/v/v) mobile phase. Then the

HPTLC plate was dried and sprayed with a reagent (10% $CuSO_3$, 8% $H_3PO_4$ aqueous solution) and heated to 180°C for 10 min and quantitated by densitometry using Image J (National Institutes of Health, Bethesda, MD, USA).

*Gas chromatography-mass spectrometry analysis*

FA species were analyzed as described previously, with slight modification [16, 17]. The free FA fraction was isolated from total lipids by HPTLC, followed by methyl esterification using odd-numbered fatty acid as an internal standard. Then derivatives were analyzed by gas chromatography (HP6890 series GC system; Hewlett Packard, Palo Alto, CA, USA)-mass spectrometry (JMS700; JEOL, Tokyo, Japan) on a Restek RTX-5 column (30 m × 0.25 mm i.d., 0.25 μm d.f.; Restek Corp., Bellefonte, PA, USA). The initial temperature was 110°C, with a 10°C increase each min, up to 300°C.

*Animals*

Seven- to ten-week-old male hairless mice (Hos: HR-1) were purchased from Hoshino Experiment Animal Center (Bando, Japan). All animal experiments were

carried out in accordance with the guidelines of, and approved by, the Animal Research Committee of Josai University.

*Induction of glycation and penetration experiments*

Skin samples removed from mice and cleaned of subcutaneous tissue and fat were mounted on vertical diffusion cells. The cells used in this study had an effective diffusion area of 1.77 $cm^2$ and a receptor compartment volume of 5.0 mL. For induction of glycation, the skin specimens were hydrated with PBS (control) or PBS containing 50 mM GO for 24 h. Glycation was induced from the basal side. The receptor fluid was maintained at 32°C, and continuously agitated with a magnetic stirrer bar.

For imaging of FL-Na penetration, skin specimens were removed from the diffusion cells after application of 1 mM of FL-Na to the SC side for 0 h, 1 h, and 6 h, and the SC surface was washed 7 times with purified water. Skin specimens were embedded in Optimal Cutting Temperature compound (Sakura Finetek Japan Co. Ltd., Tokyo, Japan), snap-frozen in liquid nitrogen, and cut into 20-μm-thick sections. All images were obtained using an IX71 microscope (Olympus, Tokyo, Japan). Signal

intensity was determined using the ImageJ Histogram tool.

*Measurement of transepidermal water loss (TEWL)*

Cutaneous water evaporation was measured with a VAPOSCAN AS-VT100RS (Asahi biomed, Yokohama, Japan). To measure excised skin, the skin surface temperature was kept at 37°C in the diffusion cells to obtain a stable TEWL value. Reconstructed epidermal models were acclimatized for 1 h before measurement.

*Measurement of skin color*

Skin color was measured using a chromameter CR-400 (Konica-Minolta, Tokyo, Japan). Measurement of skin samples was performed after placing the skin samples on a white board. Data are expressed in the L*a*b* color space, and the parameter b* was employed as the value for the yellowish tint.

*Data analysis*

Statistical differences between groups were assessed by means of Dunnett's

test or 2-tailed Student *t*-test using SAS statistics software (SAS Institute, Cary, NC, USA) and a $P$ value of $< 0.05$ was considered as the limit of statistical significance. Testing of correlation coefficients was conducted using Microsoft Excel 2011 (Redmond, WA, USA).

## RESULTS

### *The composition lipids is changed in the glycated reconstructed epidermal model*

We first evaluated the component ratio of SC intercellular lipids in the glycated epidermis. We used a reconstructed epidermal model and determined the quantity of FA, CERs, and CHOL. The content of FA in normal and 10 mM GO exposed reconstructed epidermis was 14.0 mg/cm$^2$ and 54.4 mg/cm$^2$ respectively, with GO inducing a 3.9-fold increase in FA content in glycated epidermis (Fig. 1f, $P < 0.001$). Concentration dependency was not observed in the content of various CERs or CHOL (Fig. 1a–e), thus the component ratio of intercellular lipids was changed as shown in Fig. 1g. The TEWL value increased significantly ($P < 0.001$) after 72 h of exposure to GO (Fig. 2).

*Fig. 1*

*Fig. 2*

*Glyoxal-induced glycation affects the viability of HaCaT cells*

To evaluate the effect of glycation on the skin at early stages of epidermal differentiation, we used HaCaT keratinocytes. The viability of HaCaT cells 48 h after exposure to 1.25 mM GO for 30 min was 86.2% ($P < 0.001$, Fig. 3a) and was decreased in a GO concentration-dependent manner. The fluorescence intensity derived from AGEs was significantly increased by exposure to 5 mM GO, as assessed by immunocytochemistry. This result shows that 30 min exposure to 5 mM GO was enough to induce glycation in cells 48 h after exposure (Fig. 3b and c).

*Fig. 3*

*Glycation accelerates free fatty acid production in HaCaT cells*

We next measured the content of various lengths of FA in glycated HaCaT cells. The amounts of C14:0, C16:0, C18:0, and C20:0 contained in lipid extracts from normal HaCaT cells were 0.28, 12.7, 10.0, 0.08 μg/mg (protein) respectively, while those from glycated HaCaT cells were 0.46, 27.9, 21.1, 0.12 μg/mg respectively ($P <$

0.05, $P = 0.07$, $P < 0.05$, $P < 0.05$) (Fig. 3d). These results indicate that the production of saturated FAs was accelerated by cellular glycation.

*An increase in FASN and ELOVL mRNA expression upregulates glycation-induced FA accumulation.*

To address whether the increase in FA was derived from *de novo* synthesis, we examined *FASN* and *ELOVL* mRNA expression in glycated HaCaT cells. *FASN* contributes to the production of C16, while *ELOVL* contributes to that of C<16. Of the ELOVL family, *ELOVL2* and *ELOVL3* were upregulated 18.3- and 8.9-fold respectively in glycated HaCaT cells 6 h after exposure to GO ($P < 0.001$, Fig. 4a–g). Additionally, *FASN* expression was increased 2.7-fold after 48 h GO treatment ($P < 0.05$, Fig. 4 h).

*Fig. 4*

*The excised glycated skin model has decreased inside-out and outside-in barrier functions*

The physical barrier integrity of skin was investigated using excised glycated skin to evaluate biological and physical changes in the SC. The excised glycated skin

model demonstrated a yellowish tint in a GO concentration-dependent manner (Fig. 5a). TEWL levels of each sample were measured under hydrated conditions at 37°C. Correlation between TEWL levels and $b^*$ value in glycated skin was observed as shown in Fig. 5b, but not significantly so, with r = 0.47 ($P$ = 0.07).

To determine the migration distance from the SC in normal and glycated skin, we investigated the skin penetration of FL-Na (MW: 376.28 Da). One h after application, FL-Na was distributed to the SC and observed in all layers of the skin in excised, glycated skin (Fig. 5c). In contrast, there was minimal distribution of FL-Na to the SC in normal skin. After 6 h, the distribution of FL-Na to the SC was increased in both groups. However, excised glycated skin showed higher-intensity staining, especially in the SC (Fig. 5d). These results suggest that changes in the structure of the SC by glycation disrupted barrier function and increased penetration of FL-Na across the skin.

*Fig. 5*

**DISCUSSION**

In the present study, we clarified the effect of glycation on the composition,

metabolism and barrier function of epidermal lipids. The most striking feature in the epidermal lipid profiles of glycated skin was the increase of various lengths of FAs (Fig. 1), suggesting the involvement of *de novo* synthesis of FA, via FASN and ELOVL upregulation (Fig. 4). FAs with chain lengths of up to C16 are synthesized by the FASN complex, and the ELOVL family of proteins elongates them. Among the seven mammalian homologues (ELOVL1–7), ELOVL 3 and 4 are highly expressed in skin [14, 18]. Thus, upregulation of ELOVL3 in glycated cells can explain the increase of various lengths of FAs in HaCaT cells (Fig. 3). In skin stratum granulosum, FAs are thought to be produced via $PLA_2$ from phospholipids to control skin pH [19]. In the present study, we used HaCaT cells because they represent the stratum basale of the skin. Notably, treatment with bromophenacyl bromide, an inhibitor of $PLA_2$, did not affect the FA content in HaCaT cells (data not shown). Taken together, these results suggest that FA metabolism might be differentially regulated in differentiating versus proliferating keratinocytes. Also, ceramidase or ceramide synthase activity may affect FA content. The reconstructed epidermal model will be useful to further determine the role of $PLA_2$ or other enzymes in glycated skin.

One unsolved question is why FASN and ELOVL were upregulated in glycated skin (Fig. 4). Exposure to excess glucose metabolites is known to contribute to the upregulation of lipid synthesis in many types of cells, with primary regulators of lipid synthesis including liver X receptors, sterol regulatory element-binding protein-1c, and carbohydrate response element binding protein transcription factors [20-22]. Further investigation is needed to clarify the contribution of these various pathways; however, these mechanisms may also be applicable to keratinocytes.

There are several mechanisms through which the TEWL value was affected (Fig. 2 & 5). One possible mechanism may involve changes in the physiological properties of SC intercellular lipids caused by an increasing FA to ceramide or cholesterol ratio. Another possible mechanism is cytotoxicity from saturated lipids, which were significantly increased in glycated HaCaT cells. FA-induced apoptosis is specific for the saturated FAs (C16:0 and C18:0) and does not occur with C4–C14, either saturated or unsaturated [23, 24]. Listenberger *et al.* reported that palmitate caused cell death, not via ceramide synthesis, but via reactive oxygen species (ROS) production in Chinese hamster ovary cells [12]. Consistent with this finding, our data also did not show an

increase in ceramide content; furthermore, previous studies in which ROS were generated in the advanced glycation process support the hypothesis that ROS contribute to FA-induced apoptosis in the epidermis [25].

We investigated the effect of glycation-induced alteration of the SC structure using excised skin and showed that both inside-out and outside-in barrier functions were disrupted by the induction of glycation (Fig. 5). It is well documented that percutaneous penetration occurs thorough intracellular, transcellular, and to a lesser extent, appendageal routes [26]. Notably, the major route of diffusion of hydrophilic molecules is across the polar head of the lipid. Because hydrophilic compounds show higher permeation in glycated skin, it is thought that modification of the polar head of intercellular lipids by AGEs derived from GO causes barrier disruption. This then leads to an increase in the penetration rate, as previously documented in permeation across excised, glycated skin [27]. In conclusion, not only physical changes in the epidermis, but biological alteration, especially upregulation of FA synthesis by glycation, contributed to barrier disruption. In future, inhibiting glycation and normalization of FA metabolism may offer an alternative treatment for aged or glycated skin.

## Conflicts of interest

The authors have no conflicts of interest to report.

## REFERENCES


1. Gkogkolou, Böhm M: Advanced glycation end products: Key players in skin aging? Dermatoendocrinol 2012;4:259–270.

2. Ichihashi M, Yagi M, Nomoto K, Yonei Y: Glycation Stress and Photo-Aging in Skin. Anti-Aging Medicine 2011;8:23–29.

3. Crisan M, Taulescu M, Crisan D, Cosgarea R, Parvu A, Cãtoi C, Drugan T: Expression of advanced glycation end-products on sun-exposed and non-exposed cutaneous sites during the ageing process in humans. PLoS One 2013;8:e75003.

4. Schleicher ED, Wagner E, Nerlich AG: Increased accumulation of the glycoxidation product Nε-(carboxymethyl)lysine in human tissues in diabetes and aging. J Clin Invest 1997;99:457–468.

5. Kawabata K, Yoshikawa H, Saruwatari K, Akazawa Y, Inoue T, Kuze T, Sayo T, Uchida N, Sugiyama Y: The presence of N(ε)-(Carboxymethyl) lysine in the human epidermis. Biochim Biophys Acta 2011;1814:1246–1252.

6. Sakai S, Kikuchi K, Satoh J, Tagami H, Inoue S., Functional properties of the stratum corneum in patients with diabetes mellitus: similarities to senile xerosis: Br J Dermatol 2005;153:319–323.

7. Verzijl N, DeGroot J, Thorpe SR, Bank RA, Shaw JN, Lyons TJ, Bijlsma JW, Lafeber FP, Baynes JW, TeKoppele JM: Effect of collagen turnover on the accumulation of advanced glycation end products. J Biol Chem 2000;275:39027–39031.

8. Yoshinaga E, Kawada A, Ono K, Fujimoto E, Wachi H, Harumiya S, Nagai R, Tajima S: Nε-(carboxymethyl)lysine modification of elastin alters its biological properties: implications for the accumulation of abnormal elastic fibers in actinic elastosis. J Invest Dermatol 2012;132:315–323.

9. Lohwasser C, Neureiter D, Weigle B, Kirchner T, Schuppan D: The receptor for advanced glycation end products is highly expressed in the skin and upregulated

by advanced glycation end products and tumor necrosis factor-alpha. J Invest Dermatol 2006;126:291–299.

10. Leibold JS, Riehl A, Hettinger J, Durben M, Hess J, Angel P: Keratinocyte-specific deletion of the receptor RAGE modulates the kinetics of skin inflammation *in vivo*. J Invest Dermatol 2013;133:2400–2406.

11. Zhu P, Ren M, Yang C, Hu YX, Ran JM, Yan L: Involvement of RAGE, MAPK and NF-κB pathways in AGEs-induced MMP-9 activation in HaCaT keratinocytes. Exp Dermatol 2012;21:123–129.

12. Listenberger LL, Ory DS, Schaffer JE: Palmitate-induced apoptosis can occur through a ceramide-independent pathway. J Biol Chem 2001;276:14890–14895.

13. Arner P: Insulin resistance in type 2 diabetes: role of fatty acids. Diabetes Metab Res Rev 2002;18(Suppl 2):S5–9.

14. Uchida Y: The role of fatty acid elongation in epidermal structure and function. Dermatoendocrinol 2011;3:65–69.

15. Bligh EG, Dyer WJ: A rapid method of total lipid extraction and purification. Can J Biochem Physiol 1959;37:911–917.

16. Hamanaka S, Hara M, Nishio H, Otsuka F, Suzuki A, Uchida Y: Human epidermal glucosylceramides are major precursors of stratum corneum ceramides. J Invest Dermatol 2002;119:416–423.

17. Uchida Y, Hama H, Alderson NL, Douangpanya S, Wang Y, Crumrine DA, Elias PM, Holleran WM: Fatty acid 2-hydroxylase, encoded by FA2H, accounts for differentiation-associated increase in 2-OH ceramides during keratinocyte differentiation. J Biol Chem 2007;282:13211–13219.

18. Ohno Y, Nakamichi S, Ohkuni A, Kamiyama N, Naoe A, Tsujimura H, Yokose U, Sugiura K, Ishikawa J, Akiyama M, Kihara A: Essential role of the cytochrome P450 CYP4F22 in the production of acylceramide, the key lipid for skin permeability barrier formation. Proc Natl Acad Sci USA 2015;112:7707–7712.

19. Fluhr JW, Kao J, Jain M, Ahn SK, Feingold KR, Elias PM: Generation of free fatty acids from phospholipids regulates stratum corneum acidification and integrity. J Invest Dermatol 2001;117:44–51.

20. Wang Y, Botolin D, Xu J, Christian B, Mitchell E, Jayaprakasam B, Nair MG,

Peters JM, Busik JV, Olson LK, Jump DB: Regulation of hepatic fatty acid elongase and desaturase expression in diabetes and obesity. J Lipid Res 2006;47:2028–2041.

21. Listenberger LL, Schaffer JE: Mechanisms of lipoapoptosis: implications for human heart disease. Trends Cardiovasc Med 2002;12:134–138.

22. Strable MS, Ntambi JM: Genetic control of de novo lipogenesis: role in diet-induced obesity. Crit Rev Biochem Mol Biol 2010;45:199–214.

23. Paumen MB, Ishida Y, Muramatsu M, Yamamoto M, Honjo T: Inhibition of carnitine palmitoyltransferase I augments sphingolipid synthesis and palmitate-induced apoptosis. J Biol Chem 1997;272:3324–3329.

24. de Vries JE, Vork MM, Roemen TH, de Jong YF, Cleutjens JP, van der Vusse GJ, van Bilsen M: Saturated but not mono-unsaturated fatty acids induce apoptotic cell death in neonatal rat ventricular myocytes. J Lipid Res 1997;38:1384–1394.

25. Lee C, Yim MB, Chock PB, Yim HS, Kang SO: Oxidation-reduction properties of methylglyoxal-modified protein in relation to free radical generation. J Biol Chem 1998;273:25272–25278.

26. Barry B.W: Mode of action of penetration enhancers in human skin. J. Control. Release 1987;6:85–97.

27. Yokota M, Tokudome Y: Permeation of Hydrophilic Molecules across Glycated Skin Is Differentially Regulated by the Stratum Corneum and Epidermis–Dermis. Biol Pharm Bull 2015;38:1383–1388.

**FIGURE LEGENDS**

**Figure 1** Changes in the content of epidermal lipids in the reconstructed epidermal model after 96 h exposure to glyoxal as determined by high performance thin layer chromatography: ceramide (CER)[NS] (a), CER[NP] (b), CER[AS] (c), CER[NH] (d), cholesterol (Chol) (e), fatty acid (FA) (f), and total lipid (g). All results are expressed as the mean ± S.D. of n = 3 replicates. * $P < 0.05$, ** $P < 0.01$, *** $P < 0.001$.

**Figure 2** Transepidermal water loss of the reconstructed epidermal model after 96 h exposure to glyoxal: 0 h (a), 24 h (b), 48 h (c), 72 h (d). All results are expressed as the mean ± S.D. of n = 3 replicates. *** $P < 0.001$.

**Figure 3** Viability of HaCaT cells 48 h after 30 min exposure to glyoxal as determined by MTT assay (a). Immunohistochemical analysis for advanced glycation end-products (AGEs) under the same conditions as Fig. 3a (b), the signal intensity derived from AGEs was divided by the cell number, both calculated using ImageJ (c). The content of various lengths of fatty acids as determined by gas chromatography-mass spectrometry. Lipids were extracted from HaCaT cells exposed to 0 mM (control), or 5 mM (AGEd) glyoxal (GO) for 30 min followed by 48 h incubation. (d) Cell viability is expressed as the mean ± S.D. of n = 4 replicates. The other results are the mean ± S.D. of n = 3 replicates. * $P < 0.05$, *** $P < 0.001$.

**Figure 4** Changes in the expression of fatty acid synthesis related genes as determined by real-time PCR. mRNA levels of ELOVL1–7 (a–d), and fatty acid synthase (FASN) (f), expressed as ratios to the endogenous control glyceraldehyde-3-phosphate dehydrogenase (GAPDH). All results are expressed as the mean ± S.D. of n = 3 replicates. * $P < 0.05$, *** $P < 0.001$.

**Figure 5** Inside-out and outside-in permeability across an excised glycated skin model. Macroscopic view of excised hairless mouse skin after incubation with various concentrations of glyoxal (GO) (a). Transepidermal water loss of excised skin with corresponding b* values after exposure to various concentrations of GO (b). Penetration pattern of sodium fluorescein (FL-Na) across normal and glycated skin at the indicated time points (c) and vertical intensity derived from FL-Na at an arbitrary line calculated using ImageJ (d). Glycation was induced by hydration with 50 mM of GO in PBS at 32°C or 37°C (for TEWL measurement) for 24 h.

Table S1: Sequences of primers

| gene | | sequence (5' to 3') |
|---|---|---|
| ***ELOVL1*** | Forward | TGGCACTCTCCCTCTACATTGTCTA |
| | Reverse | TGAACTTGGAGAAGAGGAAGAGC |
| ***ELOVL2*** | Forward | TCTGCTCTCAATATGGCTGGGTAA |
| | Reverse | GCGCTGGTAAGATCTTGACACTGTA |
| ***ELOVL3*** | Forward | GCCCTATAACTTCGAGCTGCTGTCCAA |
| | Reverse | CCACAGCGATGAGAACCAGGTA |
| ***ELOVL4*** | Forward | GGCATGCAGTCATGAGAATTACAGA |
| | Reverse | GGGAACCAGTACAGAATGTTCACAA |
| ***ELOVL5*** | Forward | GATTGCCTATTTACCGTTTGACAGA |
| | Reverse | TTTAGACCCTGGCAACCAGTTC |
| ***ELOVL6*** | Forward | TGCTAAGCAAAGCACCCGAAC |
| | Reverse | CAGGAGCACAGTGATGTGGTGA |
| ***ELOVL7*** | Forward | TTGGGACCAAAGCTCATGGAA |
| | Reverse | AAAGCTGTGGGTGACCGTGAATA |
| ***FASN*** | Forward | TATGCTTCTTCGTGCAGCAGTT |
| | Reverse | GCTGCCACACGCTCCTCTAG |
| ***GAPDH*** | Forward | GAAGGTGAAGGTCGGAGT |
| | Reverse | GAAGATGGTGATGGGATTTC |

# Figure 1

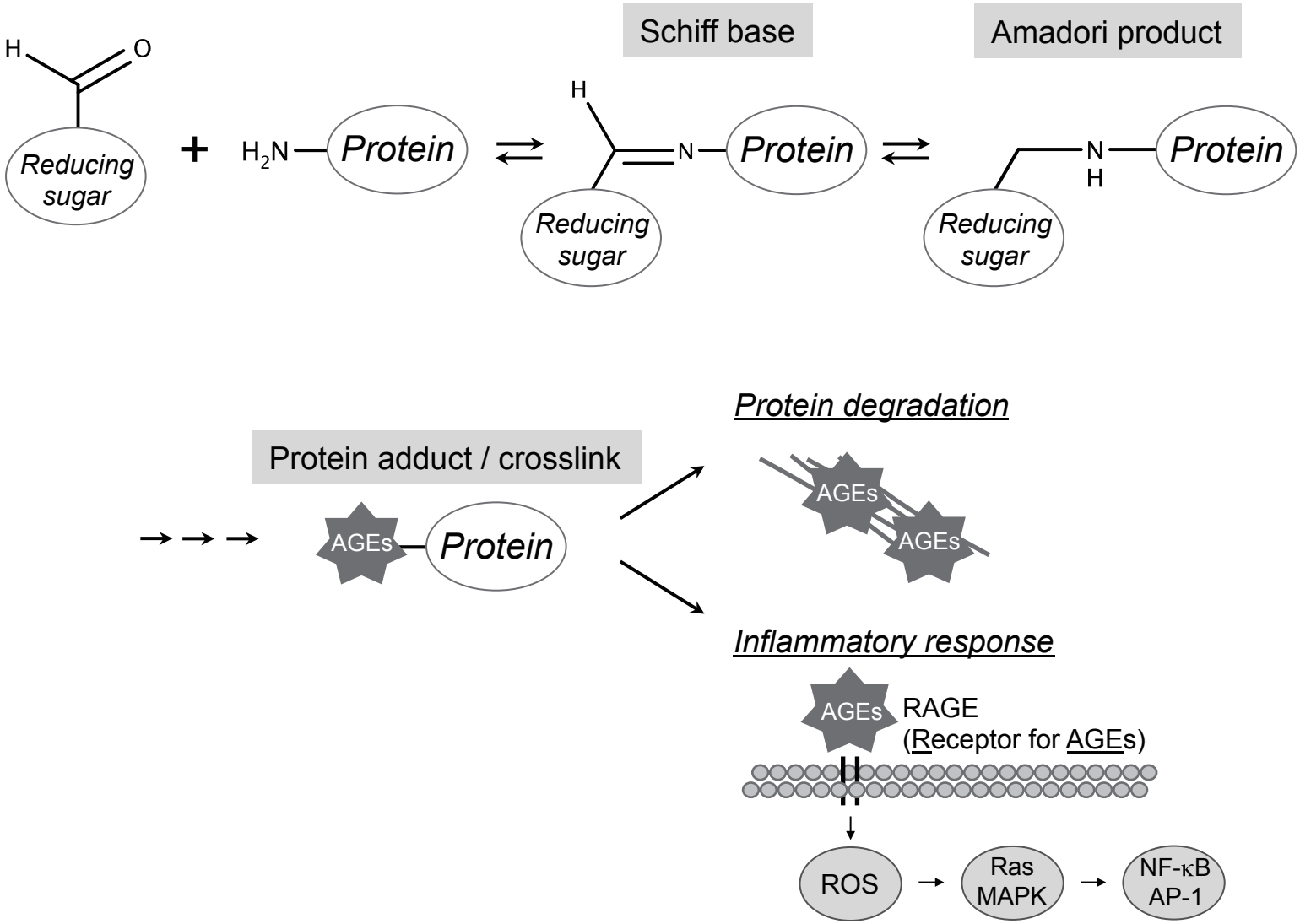
Schiff base
Amadori product
H
O
Reducing sugar
+
H2N
Protein
H
N
Protein
Reducing sugar
N
H
Protein
Reducing sugar
Protein adduct / crosslink
AGEs
Protein
Protein degradation
AGEs
AGEs
Inflammatory response
AGEs
RAGE
(Receptor for AGEs)
ROS
Ras
MAPK
NF-κB
AP-1

Figure 2

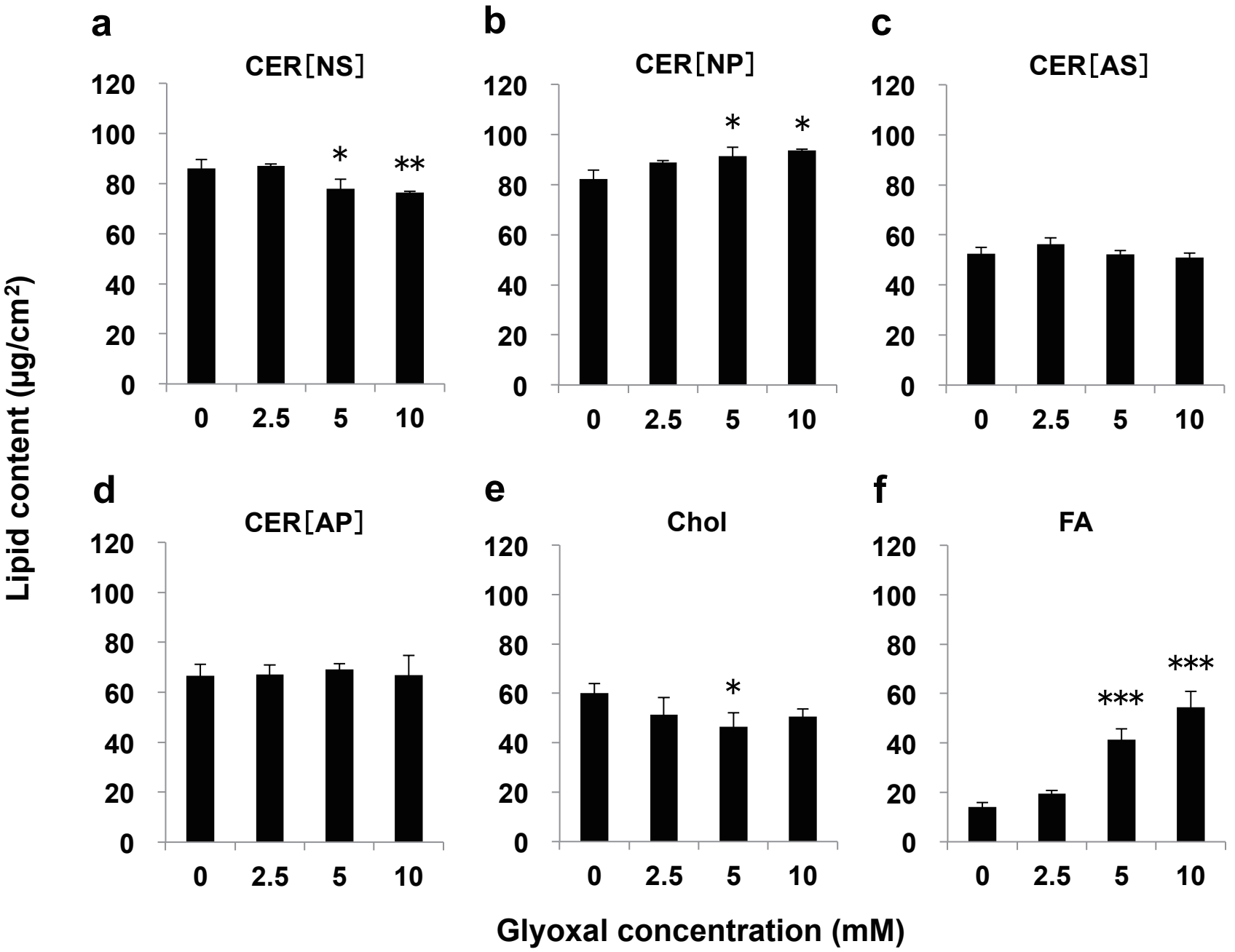
a
CER[NS]
b
CER[NP]
c
CER[AS]
d
CER[AP]
e
Chol
f
FA
Lipid content (μg/cm²)
Glyoxal concentration (mM)
0
2.5
5
10
20
40
60
80
100
120
*
**
***

# Figure 2

g

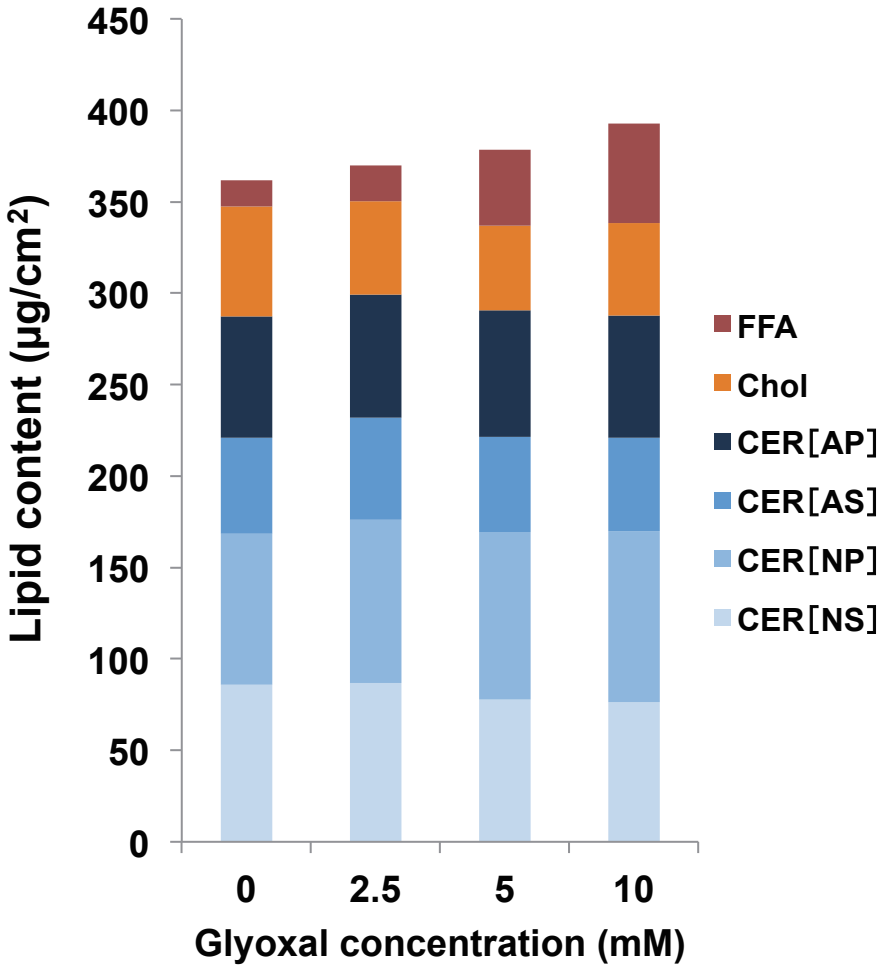
450
400
350
300
250
200
150
100
50
0
Lipid content (µg/cm²)
0
2.5
5
10
Glyoxal concentration (mM)
FFA
Chol
CER[AP]
CER[AS]
CER[NP]
CER[NS]

Figure 3

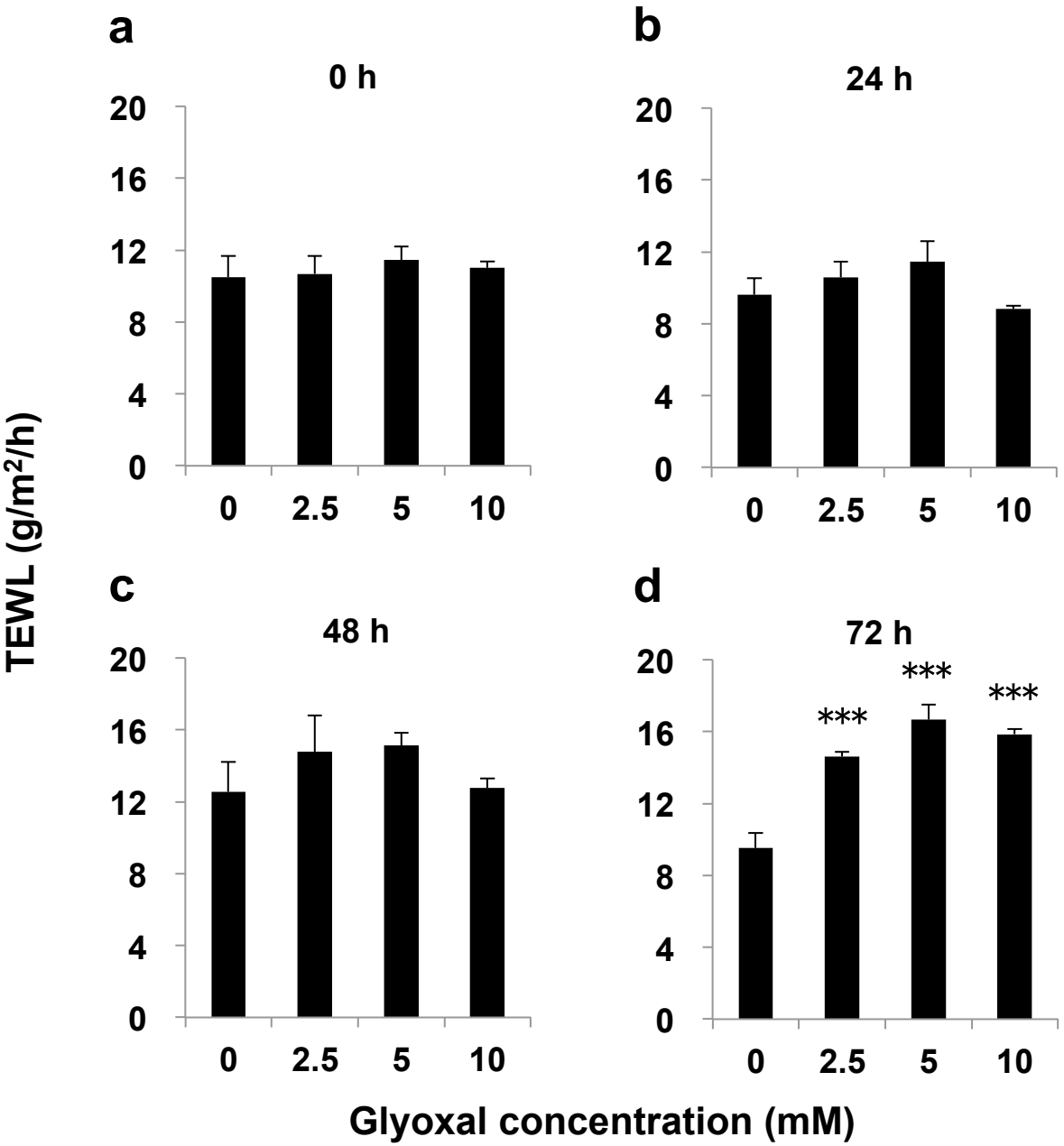
a
0 h
b
24 h
c
48 h
d
72 h
TEWL (g/m²/h)
20
16
12
8
4
0
0
2.5
5
10
***
***
***
Glyoxal concentration (mM)

# Figure 4

a

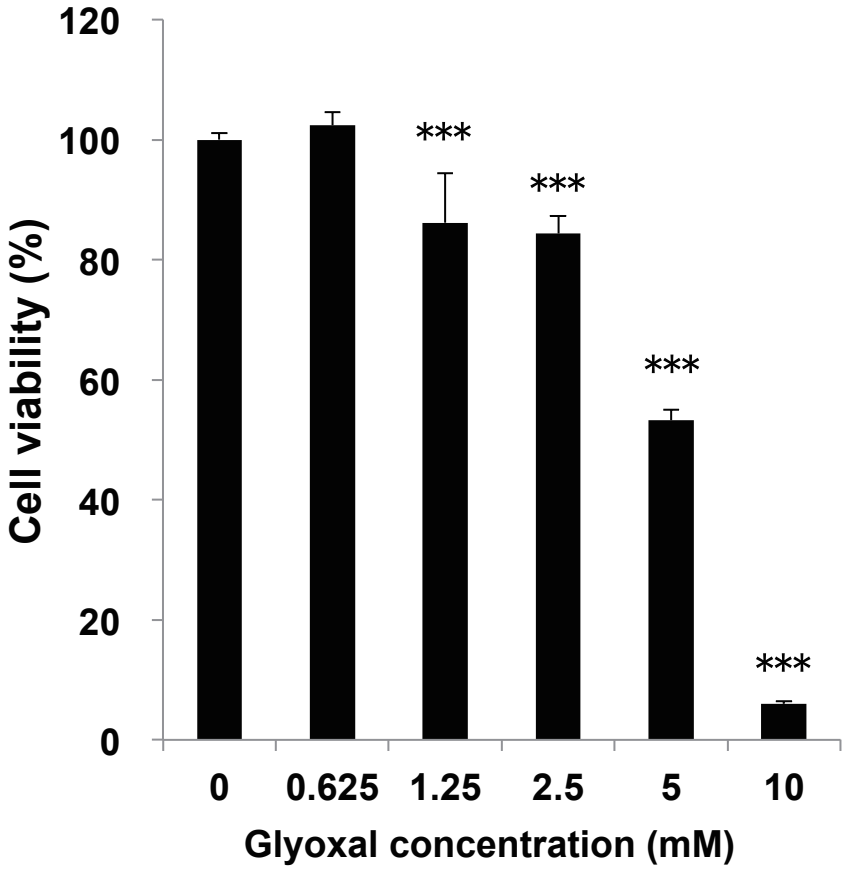
120
100
80
60
40
20
0
Cell viability (%)
***
***
***
***
0
0.625
1.25
2.5
5
10
Glyoxal concentration (mM)

# Figure 4

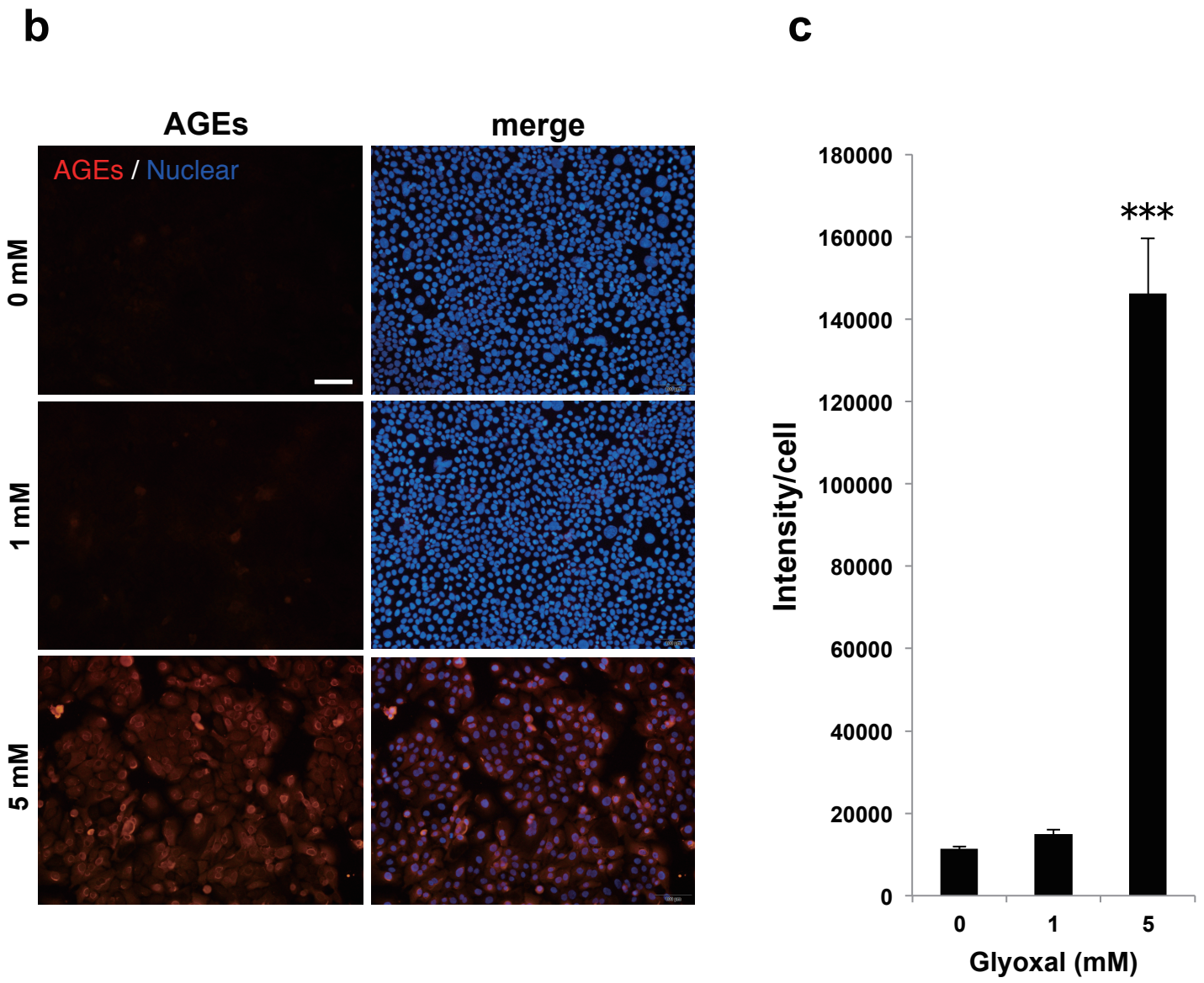
b
AGEs
merge
AGEs / Nuclear
0 mM
1 mM
5 mM
c
Intensity/cell
180000
160000
140000
120000
100000
80000
60000
40000
20000
0
***
0
1
5
Glyoxal (mM)

# Figure 4

**d**

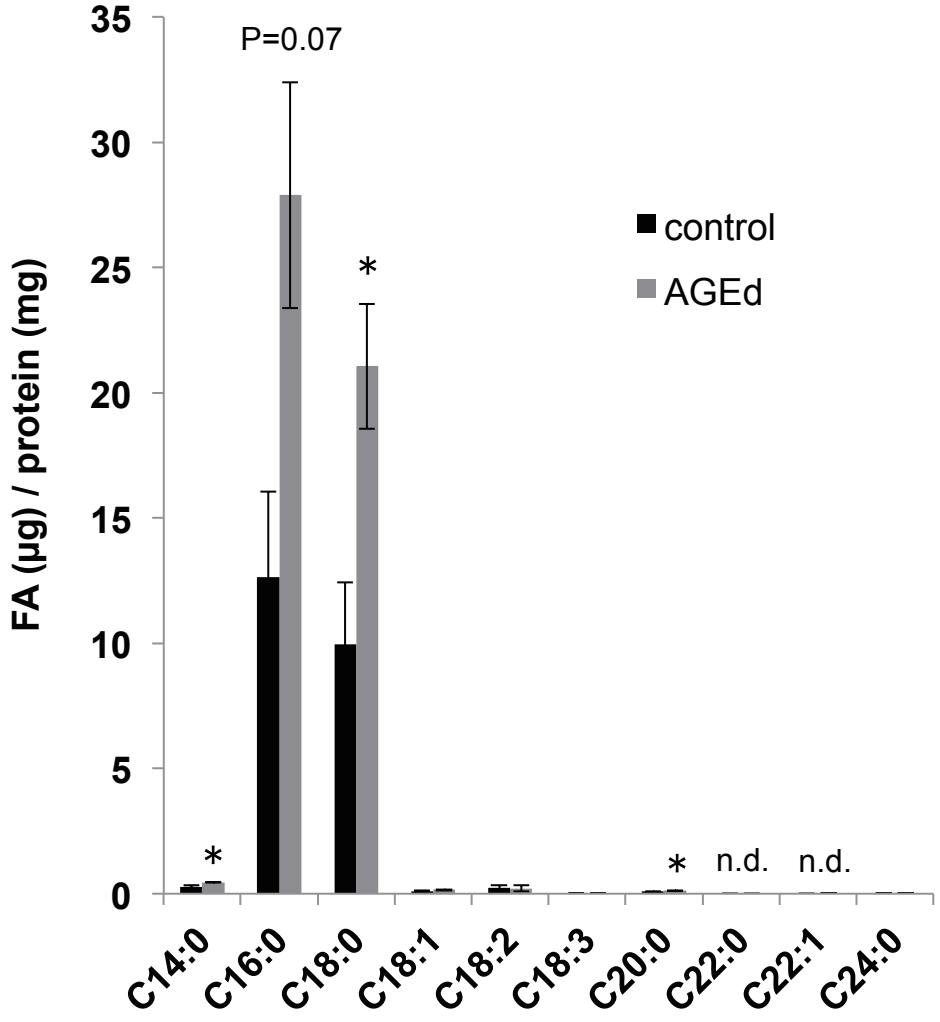
35
30
25
20
15
10
5
0
FA (µg) / protein (mg)
P=0.07
*
*
n.d.
n.d.
control
AGEd
C14:0
C16:0
C18:0
C18:1
C18:2
C18:3
C20:0
C22:0
C22:1
C24:0

# Figure 5

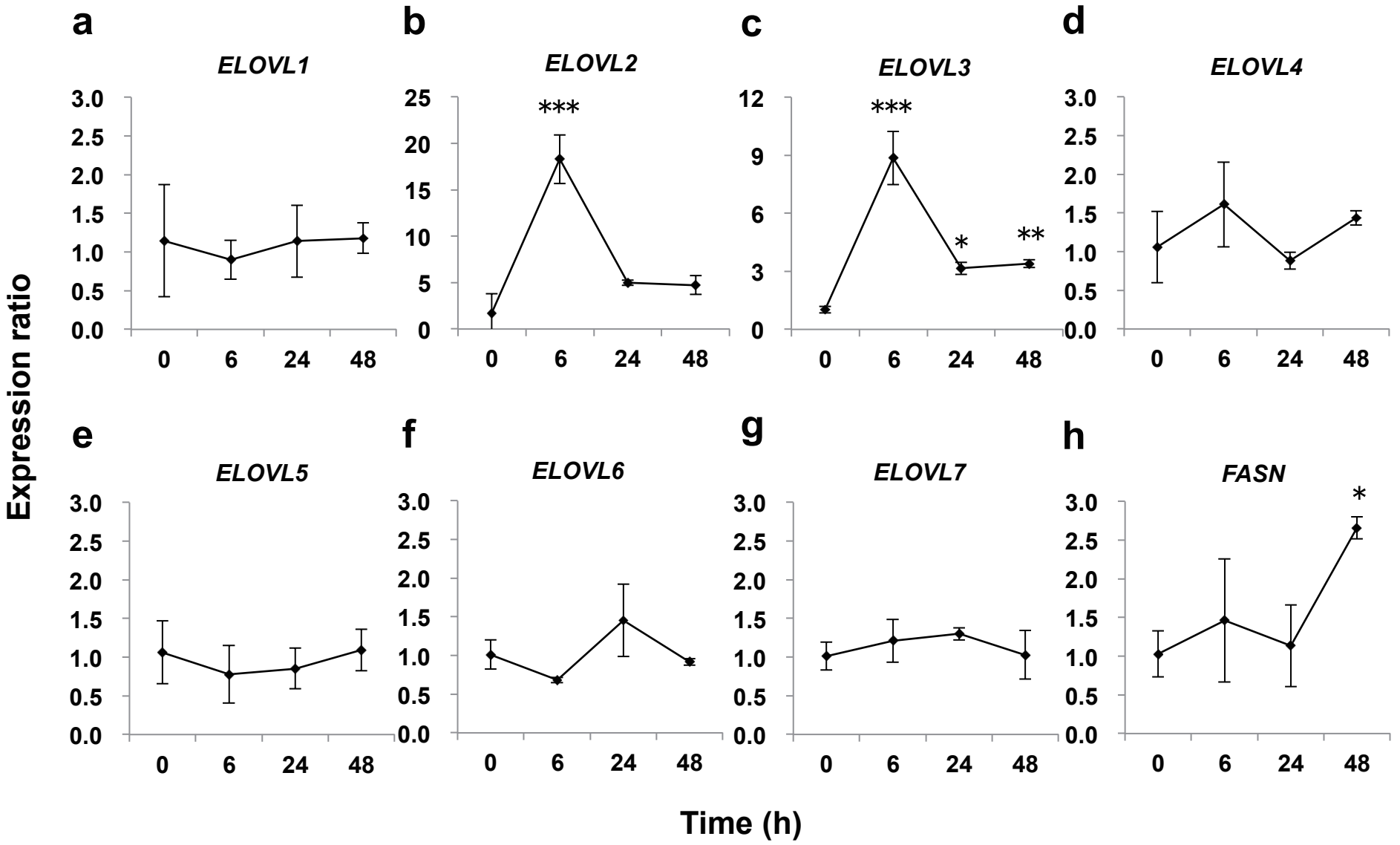
a
ELOVL1
b
ELOVL2
***
c
ELOVL3
***
*
**
d
ELOVL4
e
ELOVL5
f
ELOVL6
g
ELOVL7
h
FASN
*
Expression ratio
Time (h)
0
6
24
48

# Figure 6

**a**

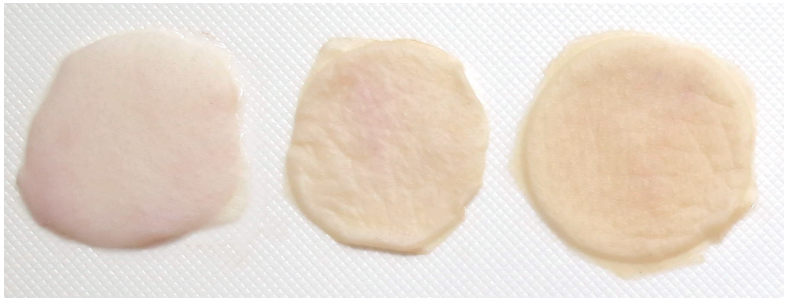

# Figure 6

**b**

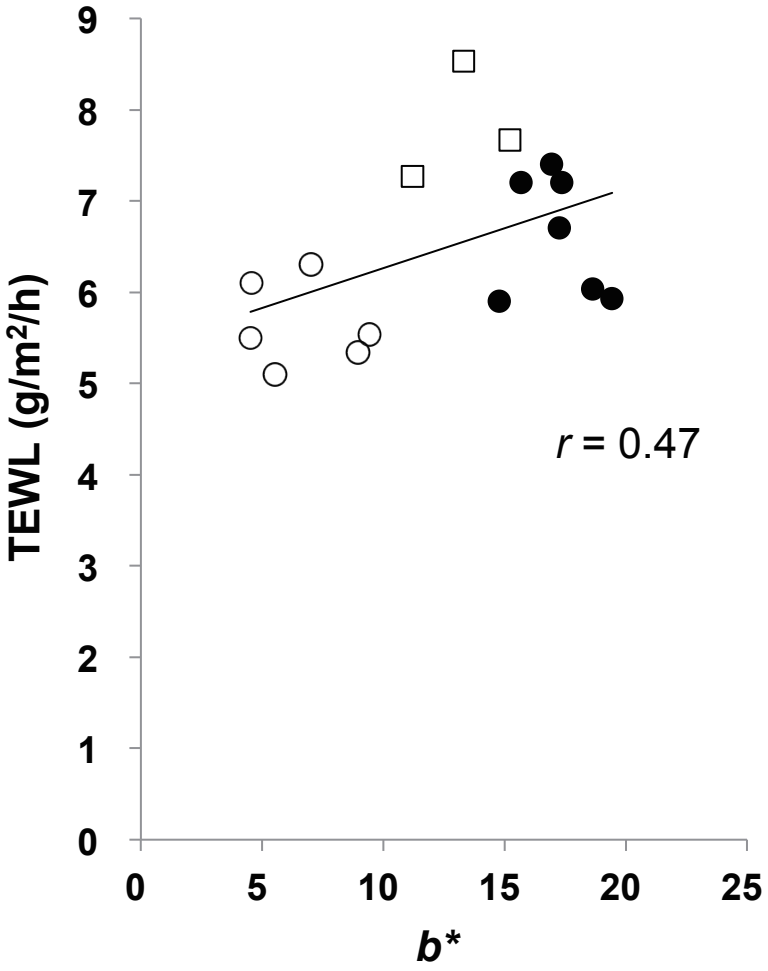

# Figure 6

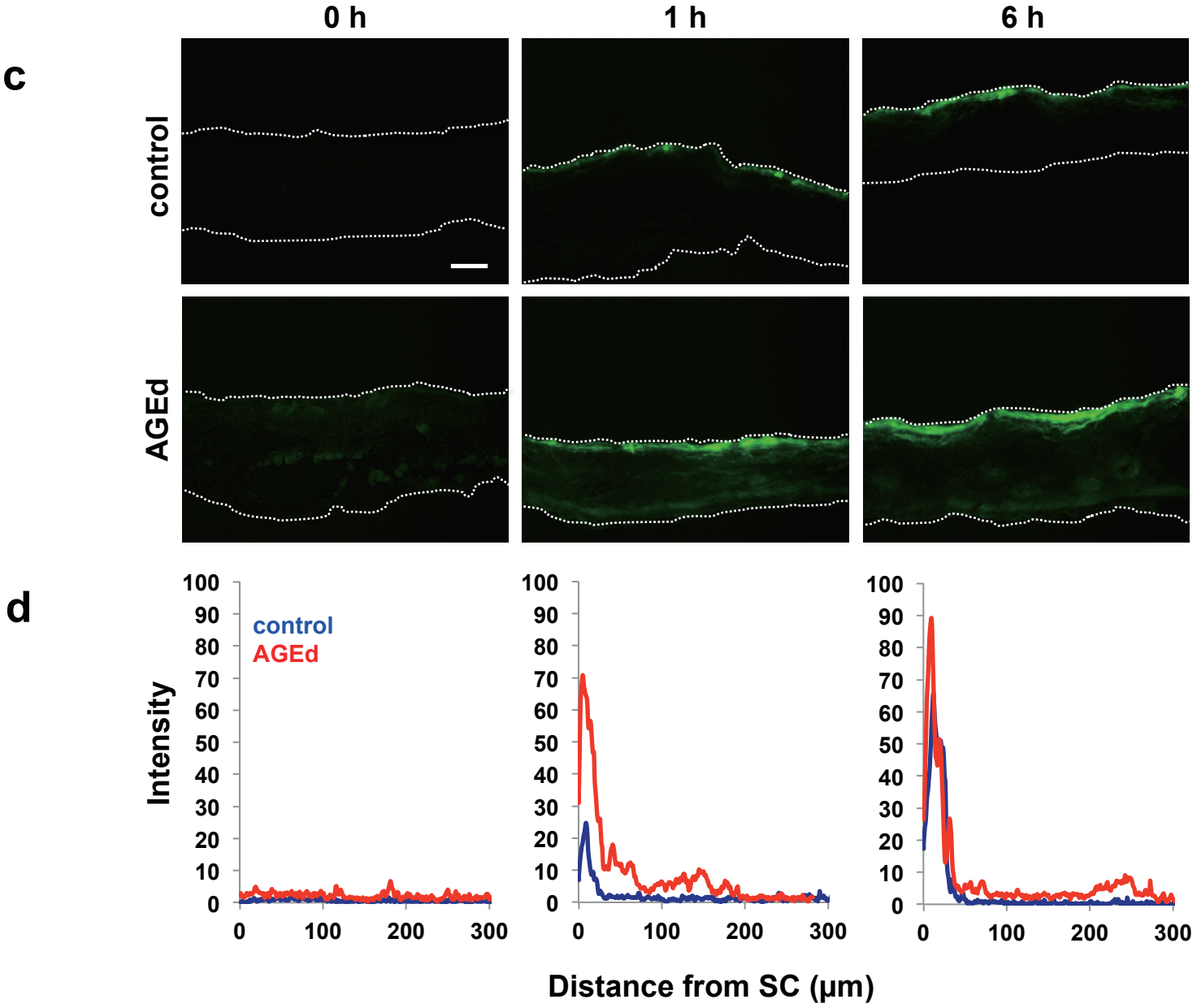
c
0 h
1 h
6 h
control
AGEd
d
control
AGEd
Intensity
100
90
80
70
60
50
40
30
20
10
0
0
100
200
300
Distance from SC (μm)

**Figure 7**

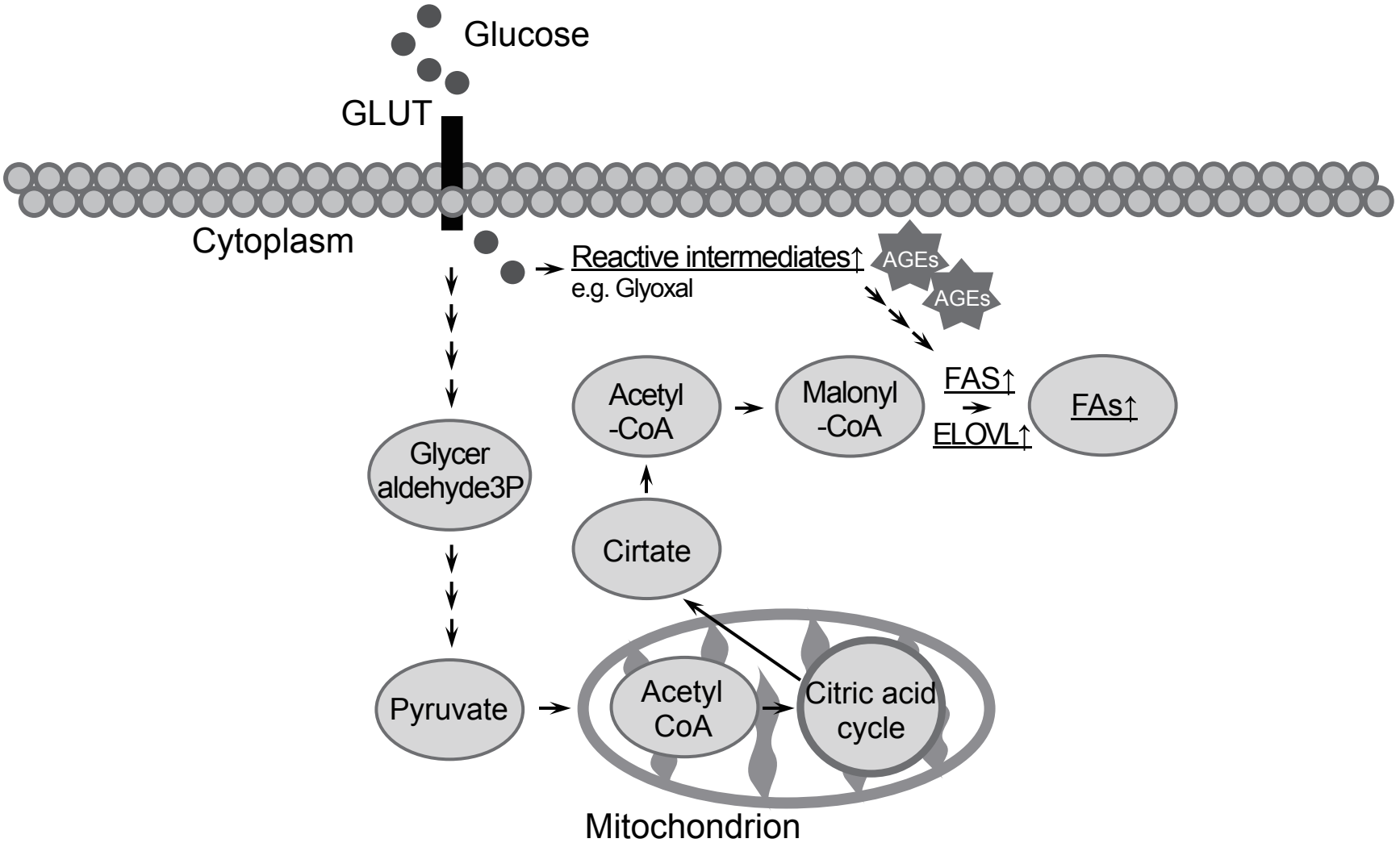
Glucose
GLUT
Cytoplasm
Reactive intermediates↑
e.g. Glyoxal
AGEs
AGEs
Acetyl
-CoA
Malonyl
-CoA
FAS↕
ELOVL↕
FAs↕
Glycer
aldehyde3P
Cirtate
Pyruvate
Acetyl
CoA
Citric acid
cycle
Mitochondrion